Modulated adiabatic passage of oriented nuclei. I. The theory

P. T. Callaghan
Department of Physics and Biophysics, Massey University, Palmerston North, New Zealand

P. J. Back and D. H. Chaplin
Department of Physics, University College, University of New South Wales, Australian Defence Force Academy, Canberra, Australian Capital Territory 2600, Australia

(Received 28 April 1987)

The anisotropic γ-ray distribution from oriented nuclei (ON) may be used to detect changes in the ensemble spin polarization and, in particular, those changes arising from nuclear magnetic resonance (NMR ON). A feature of NMR ON of dilute nuclear impurities in ferromagnets is the severe inhomogeneous broadening resulting from a distribution of magnetic hyperfine fields over the nuclear ensemble. In conventional NMR ON spectroscopy fine details of the hyperfine interaction, such as the electric quadrupole interaction, are buried in the inhomogeneous broadening. It is shown here that the quadrupole splitting may, however, be directly measured if the rf field is amplitude modulated during an adiabatic passage. Such a modulation implies a three-level coupling which is sensitive to rank-2 terms in the hyperfine Hamiltonian, and the modulation frequency corresponds to the spectral domain of the quadrupole splitting. This theory is developed and applied to nuclear ensembles with integral and half-integral spins.

I. INTRODUCTION

The anisotropic γ-ray distribution from oriented radioactive nuclei (ON) may be used to detect changes in the ensemble spin polarization. Detection of nuclear magnetic resonance via changes in γ anisotropy (NMR ON) was first demonstrated by Matthias and Holliday,[1] and since then the technique has been widely used to examine hyperfine fields at dilute impurities in a wide variety of hosts but especially ferromagnetic metals.[2]

A feature of NMR ON in ferromagnets is the presence of severe inhomogeneous broadening resulting from a distribution of magnetic hyperfine fields over the nuclear ensemble. The associated Larmor frequency spread is of order 1 MHz and in order to detect NMR ON from a significant fraction of the ensemble, it has been customary in cw spectroscopy to incoherently modulate the rf and impose a frequency spread comparable with the linewidth. In such spectroscopy (cw NMR ON) fine details of the hyperfine Hamiltonian are buried in the inhomogeneous broadening. The details which particularly concern us are the electric quadrupole interactions (EQI).

For heavy nuclear impurities the large quadrupole splittings from electric field gradients associated with the atomic local moment[3] can sometimes be resolved using frequency modulated cw NMR ON spectroscopy. Even for heavy nuclear probes, in nominally cubic ferromagnets, there are stringent requirements on sample preparation to achieve this, and to date only about 12 such systems have had their EQI directly resolved in the frequency domain.[14] Well-known examples include the ^{192}Ir*Ni* (Refs. 5–7) and ^{198,199}Au*Fe* systems (Refs. 8–11) with frequency splittings of the order of several hundred kHz. In contrast the quadrupole splittings for light impurity nuclei are merely a few kHz. Their measurement presents a rewarding challenge. Indeed a measure of these interactions, particularly their orientation dependence in single crystals, may elucidate the roles of rival mechanisms.[12] For example, do the small electric field gradients at light impurity nuclei arise from small atomic local moment effects or from the breaking of crystal cubic symmetry by magnetostriction?

Should the *total* EQI splitting $(2j-1)2P/h$ of these more difficult systems approach the inhomogeneous broadening, the EQI may be deduced in the frequency domain from small differential resonance displacements[13,14] between two γ-ray detector directions $\theta=0°$ and $\theta=90°$. The angle θ measures the angle between the magnetic hyperfine field producing the nuclear orientation and the γ-ray emission. The differential resonance displacement has its basic origin in the gross population imbalance between quadrupolar split levels at nuclear orientation temperatures, and the resulting shift is due to different weighting of the detection tensors in the cw NMR ON signals at the two detection angles.

For EQI's so small that the above frequency domain techniques are not viable it is possible to resort to time domain techniques. The classical device used in pulsed NMR is to refocus Zeeman precessions by appropriate spin-echo methods.[15] This approach has its analog in NMR ON,[16] and its application to the study of nuclear quadrupole interactions is the subject of future work. We point out, however, that the quadrupole modulations of spin echoes from high-spin nuclei (such as those employed in NMR ON) are complex and difficult to unravel. Their interpretation is particularly complicated in metallic systems by the inherent distribution of nuclear turn angles arising from the distribution of rf pulse amplitudes experienced by nuclei residing at differing depths from the metal surface.

An alternative approach is to utilize a *direct spectroscopic* determination of quadrupole splittings in a manner which is insensitive to the rf profile. A spectroscopic determination would not require a fit to the signal amplitude but instead uses the response of the spin system to an applied frequency corresponding to Hamiltonian terms of interest. In this paper we propose a spectroscopic method which achieves this object. The method is a variant of the adiabatic single-passage experiment in which the rf frequency is slowly and continuously swept through the resonant conditions.

Adiabatic single-passage experiments on oriented nuclei were first performed by Don *et al.*[17] Later Callaghan, Johnston, and Stone[18] showed that single-passage NMR ON on ^{60}Co*Fe* indicated the presence of electric quadrupole splittings smaller than the inhomogeneous broadening but larger than the rf Zeeman term. This approach again utilizes the gross population imbalance between quadrupolar split levels but here appropriate to the isochromats. As well, the technique requires the favorable long nuclear spin-lattice relaxation times that result at nuclear orientation temperatures. As long as resonant passage is effected throughout the total inhomogeneous line in a time short compared with T_1 the individual contributions from the isochromats will constructively contribute to the observed NMR ON signals. Deduction of the EQI magnitude for such *unmodulated* adiabatic passages requires time resolution of the midpassage NMR ON signal and, most importantly, detailed knowledge of the average strength of the radiofrequency field at the nuclei when fitting the time domain data.[19] This latter requirement severely restricts the accuracy of the deduced EQI using the single passage technique. The sign of the EQI may be obtained from the dependence of the postpassage signal on sweep direction.

We shall demonstrate here that the quadrupole splitting may be unambiguously determined by direct spectroscopic means if the rf field during adiabatic passage is amplitude modulated. Modulated adiabatic passage of oriented nuclei employs nuclear magnetic resonance with a signal arising from the changes in Zeeman polarization and thus has the "signal-to-noise" ratio of conventional NMR ON. But the differential response of the spin system is sensitive only to the modulation frequency applied in the regime of the quadrupole splitting. In the companion paper[20] we demonstrate the capacity of this method to measure splittings of a few kHz for Co nuclei in Fe single crystals despite the imposition of magnetic inhomogeneous broadening of order 500 kHz.

II. NUCLEAR MAGNETIC RESONANCE OF ORIENTED NUCLEI

A. Description of nuclear orientation

The distribution of the γ-ray emissions from an ensemble of radioactive nuclei is given by a product of spherical tensors[21] which transform under rotation in the usual manner

$$W(\theta)=\sum_{\nu} B_\nu U_\nu F_\nu P_\nu(\cos\theta) \ . \tag{1}$$

For the oriented ensemble in thermal equilibrium, θ represents the angle between the axis of the magnetic hyperfine field and the direction of γ emissions. The summation over ν is restricted to even values for γ-ray emission (odd-ν terms must be included in the description of the β-particle distribution). The U_ν parameters describe the reorientation effect of preceding decay transitions, and the F_ν are angular momentum coupling coefficients for the observed decay. The $P_\nu(\cos\theta)$ are Legendre polynomials.

The B_ν coefficients are sensitive to the orientation state of the parent nuclear spins. In NMR ON we detect changes in the B_ν parameters by measuring the intensity of γ emission along a fixed (e.g., $\theta=0°$) axis. The NMR ON "signal" is then given by the change in $W(0)$ from its thermal equilibrium value. A description of the NMR ON signal therefore requires an analysis of the effects on the B_ν parameter arising from the state of the nuclear ensemble.

Treatment of such systems is facilitated by using the density operator which is defined by

$$\rho=\sum_{\psi} p_\psi \, |\psi\rangle\langle\psi| \ , \tag{2}$$

where the sum is taken over the pure state subensembles with classical statistical weightings p_ψ. The average expectation value of the operator of interest A is given by

$$\langle \overline{A} \rangle = \mathrm{Tr}(\rho A) \ . \tag{3}$$

We work in the representation where the nuclear spin angular momentum operators J^2 and J_z are diagonal and characterize our eigenstates by the manifold angular momentum quantum number j and the azimuthal quantum number m. The B_ν coefficients are related to the *probability* of γ emission and are sensitive to the ensemble averaged populations comprising the diagonal elements of the density matrix ρ_{mm}. For example,

$$B_2=6\left[\frac{5(2j+1)(2j-2)!}{(2j+3)!}\right]^{1/2} \times\sum_m [m^2-\tfrac{1}{3}j(j+1)]\rho_{mm} \ . \tag{4}$$

Expressions for $\nu\geq 4$ are given elsewhere.[22]

In the NMR ON experiment the time dependence of the B_ν parameters may, therefore, be described in terms of the density matrix evolution

$$\rho(t)=U(t)\rho(0)U^\dagger(t) \tag{5}$$

with

$$i\hbar\frac{\partial}{\partial t}U(t)=\mathcal{H}U(t) \ .$$

$\mathcal{H}$ is the system Hamiltonian. In general where $\mathcal{H}$ is time dependent, $U(t)$ has a simple analytic form only for small time displacements δt

$$U(\delta t)=\exp\left[-\frac{i}{\hbar}\mathcal{H}\delta t\right] \ . \tag{6}$$

The simplest description, therefore, results from a choice of interaction representation where $\mathcal{H}$ is constant. This usually corresponds to the standard rotating-frame transformation used to describe the system evolution in nuclear magnetic resonance.

B. The nuclear hyperfine Hamiltonian

We employ a laboratory frame Hamiltonian containing an electric quadrupole interaction with principal axis Z at angle α to the direction z, of the longitudinal hyperfine Zeeman field. This magnetic interaction will always dominate the laboratory frame Hamiltonian and defines our zeroth-order representation. The rf Zeeman field $2B_1$ is applied transversely with a time dependence $f(t)$. Consider an isochromat at frequency γB_0 in the inhomogeneously broadened line of width $\gamma\Delta B_0$, where γ is the nuclear gyromagnetic ratio. In the laboratory frame

$$\mathcal{H}^L=-\hbar\gamma B_0 J_z-2\hbar\gamma B_1 f(t)J_x + P(J_z^2-\tfrac{1}{3}J^2)+P'(J_zJ_x+J_xJ_z)+P''(J_x^2-J_y^2)\ ,$$

where

$$\begin{aligned} P&=\tfrac{1}{2}(3\cos^2\alpha-1)[3eQV_{ZZ}/4j(2j-1)]\ ,\\ P'&=(\sin\alpha)(\cos\alpha)[3eQV_{ZZ}/4j(2j-1)]\ ,\\ P''&=\tfrac{1}{2}(\sin^2\alpha)[3eQV_{ZZ}/4j(2j-1)]\ . \end{aligned} \tag{7}$$

Note that where the electric field gradient possesses axial asymmetry, the secular part of the quadrupole Hamiltonian changes to[23]

$$P=[\tfrac{1}{2}(3\cos^2\alpha-1)+\eta(\sin^2\alpha)(\cos2\phi)] \times[3eQV_{ZZ}/4j(2j-1)]\ , \tag{8}$$

where η is the asymmetry parameter defined by

$$\eta=\frac{V_{XX}-V_{YY}}{V_{ZZ}} \tag{9}$$

and ϕ is the azimuth angle relating the (X,Y,Z) and (x,y,z) frames.

Our chosen Hamiltonian contains spin tensors up to rank two. We will find it instructive to expand $\mathcal{H}$ in a basis of a rank 0, 1, and 2 Cartesian tensors such that

$$\mathcal{H}=H_0 I+\sum_{l=x,y,z} H_l J_l+\sum_{m,n=x,y,z} H_{mn}T_{mn}\ . \tag{10}$$

The rank-2 tensors are described in the Appendix.

C. Single-passage NMR ON-unmodulated rf

We first review the adiabatic single-passage experiment for unmodulated rf. For this "pure carrier" case, $f(t)=\cos(\omega t)$ and the time-dependent transverse-field term may be decomposed into separate rotating and counter rotating components via

$$2\gamma B_1 J_x\cos(\omega t)=\gamma B_1[J_x\cos(\omega t)+J_y\sin(\omega t)] +\gamma B_1[J_x\cos(\omega t)-J_y\sin(\omega t)]\ . \tag{11}$$

In the frame rotating at ω about the z axis, the diagonal term $\gamma B_0 J_z$ is reduced by ωJ_z while one rotating-field term becomes stationary. The rapidly oscillating counterrotating field may be neglected. The resulting evolution under the influence of now static off-diagonal terms constitutes the resonance phenomenon, the resonant frequency corresponding to that which renders the diagonal elements of the Hamiltonian zero. We are here concerned with the influence of the quadrupole interaction in lifting the Zeeman degeneracies.

In a passage experiment in which ω is swept from far below to far above resonance, pairs of diagonal elements of $\mathcal{H}$ become degenerate in succession. Hence only pairs of levels interact, and we may treat these "submanifold" pairs of "substates" in a pseudo-spin-$\frac{1}{2}$ formalism.[18] In the laboratory frame, the submanifold pair $|m+1\rangle$, $|m\rangle$ has effective Hamiltonian

$$\mathcal{H}^L=H_0^L I+H_x^L J_x+H_y^L J_y+H_z^L J_z\ , \tag{12}$$

where the scalar coefficients are defined as

$$\begin{aligned} H_0^L&=-\hbar\gamma B_0(m+\tfrac{1}{2})+P\{\tfrac{1}{2}[(m+1)^2+m^2]-\tfrac{1}{3}j(j+1)\},\\ H_x^L&=-\hbar\gamma B_1 k_m\cos(\omega t)+P'k_m(2m+1)\ ,\\ H_y^L&=-\hbar\gamma B_1 k_m\sin(\omega t)\ ,\\ H_z^L&=-\hbar\gamma B_0+P(2m+1)\ , \end{aligned} \tag{13}$$

and

$$k_m=[j(j+1)-m(m+1)]^{1/2}\ . \tag{14}$$

I is the identity matrix.

The term $H_0^L I$ serves only to shift the entire submanifold energy and may be neglected. The extra term in H_x^L arising from the quadrupole interaction oscillates at the Larmor frequency in the rotating frame, and its effect averages to zero. Transformation to the rotating frame yields

$$\begin{aligned} &H_0^R=H_0^L,\quad H_x^R=-\hbar\gamma B_1 k_m\ ,\\ &H_y^R=0,\quad H_z^R=-\hbar\gamma(B_0-\omega/\gamma)+P(2m+1)\ . \end{aligned} \tag{15}$$

Subresonance occurs when H_z^R is close to zero.

We shall here be concerned only with the case $\hbar\gamma B_1 k_m<P\ll\hbar\gamma B_0$. It is apparent that the effective rf field amplitude at each subresonance is given by $B_1 k_m$. Thus, provided $\hbar\gamma B_1 k_m\ll P$, each subresonance is well separated, and the successive density matrix evolutions are entirely equivalent to those of spin-$\frac{1}{2}$ systems. Figure 1 illustrates this phenomenon. To understand the evolution of the density matrix during passage, we look for a reference frame in which the Hamiltonian is diagonal and the populations stationary. Such a frame is the effective field direction illustrated in Fig. 2. The small off-diagonal Hamiltonian term is of order $\hbar(d\theta/dt)J_y$ and may be neglected provided

$$\frac{d\omega}{dt}\ll(\gamma B_1 k_m)^2\ . \tag{16}$$

This corresponds to the so-called adiabatic condition. The effective adiabatic parameter

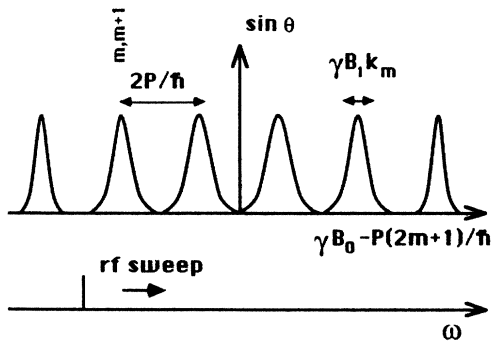

FIG. 1. Response of spin system to transverse rf field $2B_1\cos(\omega t)$ as ω as varied. The Lorentzian curves correspond to the family of subresonances in the $|m\rangle$, $|m+1\rangle$ submanifolds. The ordinate is given by the effective field direction as defined in Fig. 2. Each subresonance has width $\gamma B_1[j(j+1)-m(m+1)]^{1/2}$ and pairs of subresonances are separated by $2P/\hbar$.

$$A_m=(\gamma B_1 k_m)^2/(d\omega/dt)$$

for each submanifold gives an indication of the extent to which the density matrix remains constant in the effective field frame. In the rotating frame the successive evolutions of the pseudo-spin-$\frac{1}{2}$ systems for $A_m \gg 1$ corresponds to rotations by π.

For $A_m \gg 1$ each submanifold pair experiences a "population inversion" as the rf field is swept through subresonance. The effect of each two-level subresonance is a successive cyclic permutation of the first accessed substate population with the populations of higher substates. Although different isochromats in the inhomogeneously broadened line experience asynchronous subresonances, the net result of the successive population inversion in a complete sweep is a cyclic population shift. At passage completion the first accessed population has been carried through to the last substate. The gross signal asymmetry depending on sweep sense is due to the nuclear orientation effect, and this result is independent of the inhomogeneous linewidth provided relaxation effects are neglected. Ideally adiabatic passage is performed sufficiently rapidly for relaxation effects to be ignored. Under such circumstances it is termed "fast passage." In adiabatic passage experiments on oriented nuclei in metallic ferromagnets at millikelvin temperatures, the relaxation times are many seconds. It is accurate to assume that each isochromat experiences fast passage. However, because of the finite time taken to sweep through the broadened line, the effects of asynchronous postpassage relaxation may be apparent.

Figure 3 compares the results of different sweep directions. It is well known that this sweep dependence of the final ensemble density matrix yields the sign of the electric quadrupole interaction.[24] For $(d\omega/dt)P<0$ the lowest population is accessed first, and this cyclic shift leads to the larger change in the B_ν parameters. The ability of the single-passage experiment to give the *sign* of P is independent of broadening. However, where the inhomogeneous linewidth $\gamma\Delta B_0$ exceeds the quadrupole splitting $P/\hbar$, the broadening obscures the magnitude of the splitting in the single-passage experiment just as it obscures the splitting in the conventional NMR ON spectrum. It is the problem of accurately determining the magnitude of the quadrupole interaction which concerns us here.

Callaghan, Johnston, and Stone[18] have shown that single passage may be used to determine the quadrupole interaction magnitude where P is not too small. For $P/\hbar<\gamma\Delta B_0$ the time dependence of the signal during passage (midpassage structure) can, if sufficiently well resolved, be fitted to yield P provided B_1 is known for all nuclei, a condition which is exceedingly difficult to satisfy in NMR ON. Lattimer[25] discusses in considerable detail the developments and complexities of the unmodulated single-passage NMR ON curve-fitting procedures required to extract a quadrupole interaction magnitude

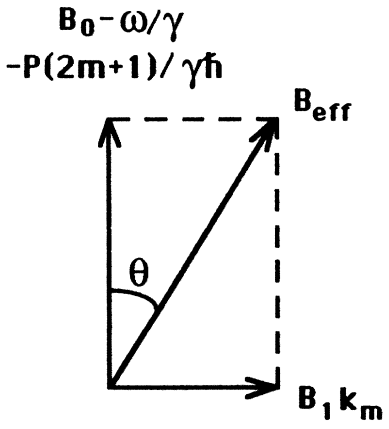

FIG. 2. Effective field direction for the pseudo-spin-$\frac{1}{2}$ Hamiltonian of the $|m\rangle$, $|m+1\rangle$ submanifold in the frame rotating at ω. As ω is varied under adiabatic conditions, the Hamiltonian may be diagonalized along the effective field direction.

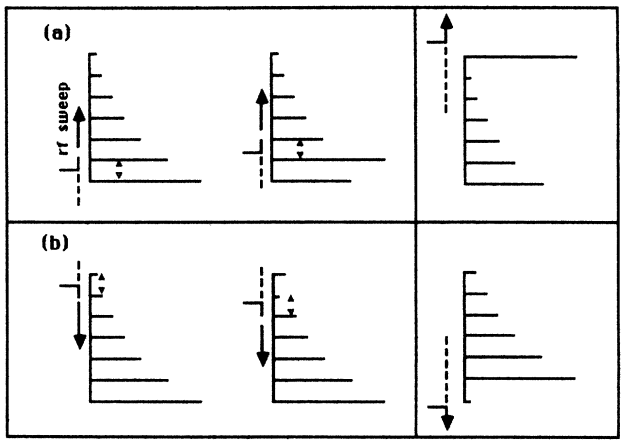

FIG. 3. Adiabatic single-passage (unmodulated rf) through quadrupole separated subresonances showing cyclic permutation of sublevel populations for the passage first entering (a) most populated, (b) least populated levels.

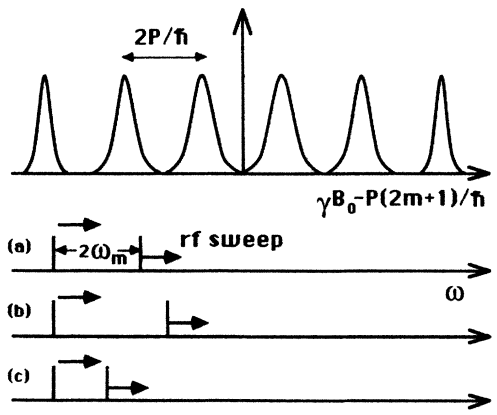

FIG. 4. Influence of modulated rf sidebands on the excitation spectrum of the spin system. In case (a) where the rf fields couple three levels simultaneously, the pseudo-spin-$\frac{1}{2}$ description fails. For well-separated interactions as in (b) for $\omega_m > P/\hbar$ and (c) for $\omega_m < P/\hbar$, successive pseudo-spin-$\frac{1}{2}$ inversions can be envisaged.

from the time resolved midpassage signals. The major systematic error in the deduction of the magnitude stems from the sensitivity to the rf field profile over the diffusion profile of the resonating radioactive impurity nuclei. The fit is subject to the limitation that the all-important midpassage structure of the sweep direction entering the most populous substate first is not always resolved.[25] The structure is easily lost for excessive inhomogeneous broadening, fast relaxation, or a distribution of quadrupole frequencies.

D. Single-passage NMR ON: Modulated rf

A determination of P independent of a knowledge of the rf field strength requires a direct spectroscopic measure of the splitting. The defect in the pure carrier single passage is then apparent. The pseudo-spin-$\frac{1}{2}$ nature of the subresonance interactions denies access to rank-2 tensor terms in the lab frame Hamiltonian.

For the quadrupole splitting to directly influence the sublevel population transfers, the subresonance Hamiltonian must be at least rank 2. This implies at least a three-level coupling, a result which is achieved by the simultaneous imposition of *two* rf fields. The separation frequency of these fields then gives a spectroscopic domain which directly probes the quadrupole splitting.

Suppose $f(t)$ in Eq. (6) corresponds to an amplitude modulated rf field with total carrier suppression. Then

$$f(t)=\cos(\omega t)\cos(\omega_m t)\ , \tag{17}$$

where ω_m is the modulation frequency. In the frequency domain the rf field consists of the two side bands shown in Fig. 4 in which the excitation spectrum is illustrated for $\omega_m \sim P/\hbar$. A simplified description of this phenomenon is given by considering two identical conventional fast passages performed in very close succession in the same direction. For $\omega_m > P/\hbar$ the modulated passage results in a distinctive reorganization of sublevel populations in which a net population transfer of the first *two* accessed substate populations is cyclically permuted through to the final two substates in much the same fashion as unmodulated single passage. For $\omega_m < P/\hbar$, however, the successive double transits through each subresonance yields a null result, and the post passage signal is zero. These are illustrated in Fig. 5. In the limit $\omega_m < \gamma B_1$ the adiabatic passage reduces to the case of the pure carrier, the cyclic population shift. We expect, therefore, that as ω_m is varied the spectrum of $P/\hbar$ will be directly revealed with an effective linewidth $\gamma B_1 \overline{k_m}$, where $\overline{k_m}$ represents the appropriate average over all subresonances. This experiment we call modulated adia-

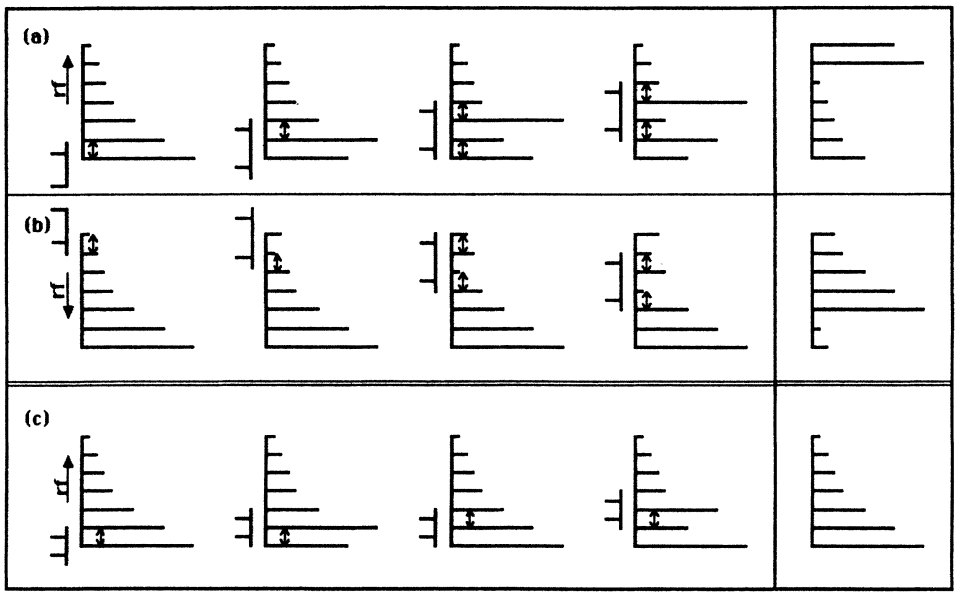

FIG. 5. Modulated adiabatic passage through subresonances in the well-separated cases of Figs. 4(b) and 4(c) in which successive inversions apply. The figure illustrates separate cyclic permutation of sublevel populations for each component sideband for passage first entering (a) most populated $\omega_m > P/\hbar$, (b) least populated $\omega_m > P/\hbar$, (c) most populated $\omega_m < P/\hbar$.

batic passage of oriented nuclei (MAPON).

Of course, it is not necessary that full adiabaticity or substate population inversion is achieved. Whatever the population reorganization resulting from the leading frequency component, the trailing frequency will still produce measurable differences depending on the frequency separation relative to $P/\hbar$. The magnitude of the adiabatic parameter is not part of the fitting routine, and the magnitude of $P/\hbar$ is read directly as a frequency "off the abscissa" as is the case for frequency resolved cw NMR ON.

III. CALCULATION OF THE MAPON LINE SHAPE

A. Description of the submanifolds

The response of the postpassage nuclear orientation parameters as the modulation frequency is varied through $P/\hbar$ gives the MAPON line shape. At the line "center" where $\omega_m \sim P/\hbar$, the substate population evolution involves three substates simultaneously. This dictates the size of our submatrix representation. In Fig. 4 it is apparent that with the exception of the first and last excitations in the sweep, the modulated passage subresonances involve three levels and are described in a spin-one formalism.

In our description we presume that no other more distant eigenstates are participating. In other words $\gamma B_1 k_m < P/\hbar$, a realistic constraint given that $\gamma B_1 k_m$ is our "linewidth" and $P/\hbar$ our "quadrupole resonance frequency in modulation frequency space."

We may now trace the method of Eqs. (12)–(15) and write for the laboratory frame in the $|m+1\rangle$, $|m\rangle$, $|m-1\rangle$ submanifold.

$$
\begin{aligned}
H_0^L &= -\hbar\gamma B_0 m + P[m^2 + \tfrac{2}{3} - \tfrac{1}{3}j(j+1)] , \\
H_x^L &= -\hbar\gamma B_1 \frac{1}{2\sqrt{2}}(k_m + k_{m-1})\cos(\omega t)\cos(\omega_m t) \\
&\quad + P' \frac{1}{2\sqrt{2}}[k_m(2m+1) + k_{m-1}(2m-1)] , \\
H_y^L &= -\hbar\gamma B_1 \frac{1}{2\sqrt{2}}(k_m + k_{m-1})\sin(\omega t)\cos(\omega_m t) , \\
H_z^L &= -\hbar\gamma B_0 + P2m , \\
H_{zz}^L &= (\tfrac{2}{3})^{1/2} P , \\
H_{xz}^L &= -\hbar\gamma B_1 \tfrac{1}{2}(k_m - k_{m-1})\cos(\omega t)\cos(\omega_m t) \\
&\quad + P' \tfrac{1}{2}[k_m(2m+1) + k_{m-1}(2m-1)] , \\
H_{yz}^L &= -\hbar\gamma B_1 \tfrac{1}{2}(k_m - k_{m-1})\sin(\omega t)\cos(\omega_m t) , \\
\frac{H_{xx-yy}^L}{\sqrt{3}} &= \frac{1}{\sqrt{2}} k_m k_{m-1} P'' , \\
H_{xy}^L &= 0 .
\end{aligned}
\tag{18}
$$

The Cartesian tensors for pseudo-spin-1 are defined in the Appendix.

For the frame rotating about the z axis at ω,

$$
\begin{aligned}
H_0^R &= -\hbar\gamma B_0 m + P[m^2 + \tfrac{2}{3} - \tfrac{1}{3}j(j+1)] , \\
H_x^R &= -\hbar\gamma B_1 \frac{1}{2\sqrt{2}}(k_m + k_{m-1})\cos(\omega_m t) , \\
H_y^R &= 0 , \\
H_z^R &= -\hbar\gamma(B_0 - \omega/\gamma) + P2m , \\
H_{zz}^R &= (\tfrac{2}{3})^{1/2} P , \\
H_{xz}^R &= -\hbar\gamma B_1 \tfrac{1}{2}(k_m - k_{m-1})\cos(\omega_m t) , \\
H_{yz}^R &= H_{xy}^R = \frac{H_{xx-yy}^L}{\sqrt{3}} = 0 .
\end{aligned}
\tag{19}
$$

All terms oscillating at the Larmor frequency have been rejected. For the modulated passage analysis we face an immediate problem. In the rotating frame our Hamiltonian is nonstatic. Furthermore, in order to yield a diagonal $\mathcal{H}$, our instantaneous (effective field) frame must reorient with time at frequency ω_m under the adiabatic condition $\gamma B_1 \gg \omega_m$. This is clearly not a region of interest. We do not observe a simple pseudo-spin-1 inversion and are bound to calculate the ensemble evolution operator from first principles if we are to follow the system evolution.

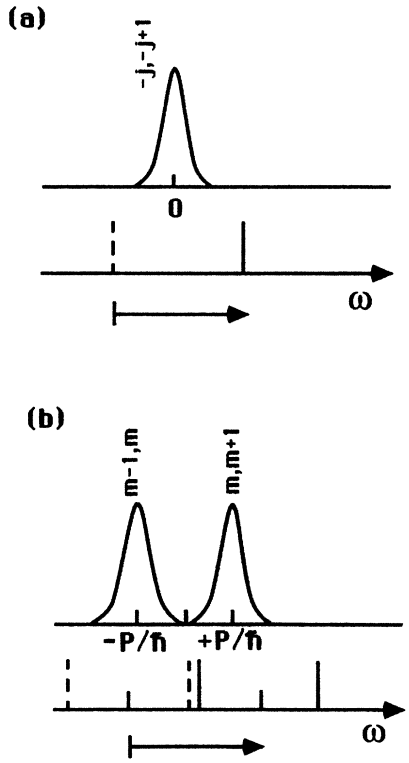

FIG. 6. Subresonance and submanifold description for MAPON with centered frequency. (a) The effect of the first and last subresonance in which a single sideband is involved. The computed result is entirely equivalent to the pseudo-spin-$\frac{1}{2}$ case with $\omega_m = 0$ and rf amplitude $\frac{1}{2}B_1$. (b) The double sideband sweep in which three sublevels $|m-1\rangle$, $|m\rangle$, and $|m+1\rangle$ are coupled. The suppressed carrier ω is varied between $\pm P/\hbar$.

B. The subresonance evolution matrices

Because our Hamiltonian is time dependent in all frames of physical interest, we are denied a simple analytic solution since this relies on our finding an interaction representation where $\mathcal{H}$ becomes stationary. We are, therefore, condemned to evolve our system continuously using the incremental evolution operator of Eq. (6). The evaluation is, however, considerably simplified by working in successive spin-one submanifolds and not in $(2j+1)$-dimensional space. Figure 6 illustrates the nature of the $2j+1$ successive evolutions to be determined, the first and last being in spin-$\frac{1}{2}$-like [Fig. 6(a)] and the rest in spin-1 like submanifolds [Fig. 6(b)].

The evolution operators to be calculated for each subresonance are coherent within a given isochromat. However, inhomogeneous broadening means that different isochromats undergo particular subresonances at different times. This implies a random phase distribution between like subresonances in different isochromats across the entire ensemble. We may express this algebraically. Let us describe our isochromats by their local offset frequency $\Delta\omega$ from the center of the inhomogeneously broadened line. The classical weighting of the isochromat is then $p(\Delta\omega)$. We will work in a rotating frame representation corresponding to an isochromat at the line center.

Consider the evolution of the ensemble density matrix over a time $t_i - t_f$:

$$\rho(t_f) = U(t_f - t_i)\rho(t_i)U^{\dagger}(t_f - t_i) = \int p(\Delta\omega) U_{\Delta\omega}(t_f - t_i)\rho_{\Delta\omega}(t_i)U^{\dagger}_{\Delta\omega}(t_f - t_i)\, d\Delta\omega \ , \tag{20}$$

where $\rho_{\Delta\omega}(t_i)$ is the density matrix of the $\Delta\omega$ isochromat at time t_i.

$U_{\Delta\omega}(t_f - t_i)$ is the evolution operator for the $\Delta\omega$ isochromat. In the rotating frame at the line center

$$U_{\Delta\omega}(t_f - t_i) = \exp[-iJ_z\Theta(\Delta\omega)]U(\mathrm{sr})\exp[iJ_z\Theta(\Delta\omega)] \ , \tag{21}$$

where $\Theta(\Delta\omega)$ refers to the z-axis rotation transforming the local isochromat rotating frame to the line center isochromat frame. $U(\mathrm{sr})$ is a subresonance evolution operator common to all isochromats.

Suppose we start with an ensemble in equilibrium. Then the diagonal $\rho_{\Delta\omega}(0)$ are effectively identical for all isochromats (given $\Delta B_0/B_0 \ll 1$) and simply equal $\rho(0)$

$$\rho(0) = \frac{1}{Z}\begin{bmatrix} \exp(-jB_0\hbar/kT) & & & \\ & \ddots & & \\ & & \exp(-mB_0\hbar/kT) & \\ & & & \ddots \\ & & & & \exp(jB_0\hbar/kT) \end{bmatrix}$$

and

$$Z = \sum_{m=-j}^{j} \exp(-mB_0\hbar/kT) \ . \tag{22}$$

It is apparent that the ensemble density matrix will then remain diagonal in a sweep through the line because all off-diagonal elements will decay with a time constant related to the inhomogeneous linewidth. This result arises from the average of $\Delta\omega$ in Eq. (20) as follows.

Consider the (m,k)th element of ρ at time t_f given that ρ is diagonal at t_i. Then

$$\begin{aligned} \rho_{m,k}(t_f) &= \int p(\Delta\omega)\sum_n U_{mn}(t_f - t_i)\rho_{n,n}(t_i)U^{\dagger}_{nk}(t_f - t_i)\, d\Delta\omega \\ &= \int p(\Delta\omega)\sum_n \exp[-im\Theta(\Delta\omega)]U_{mn}(\mathrm{sr})\exp[-in\Theta(\Delta\omega)]\rho_{n,n}(t_i)\exp[in\Theta(\Delta\omega)]U^{\dagger}_{nk}(\mathrm{sr})\exp[ik\Theta(\Delta\omega)]\, d\Delta\omega \\ &= \int p(\Delta\omega)\sum_n \exp[-i(m-k)\Theta(\Delta\omega)]U_{mn}(\mathrm{sr})\rho_{n,n}(t_i)U^{\dagger}_{nk}(\mathrm{sr})\, d\Delta\omega \ , \end{aligned} \tag{23}$$

but unless $m=k$, $\exp[-i(m-k)\Theta(\Delta\omega)]$ averages to zero over a time scale given by the inverse inhomogeneous linewidth. Therefore,

$$\rho_{m,k}(t_f) = 0, \quad m \neq k \ . \tag{24}$$

Hence, to calculate the effects of successive subresonances we need follow only the evolution of the diagonal elements of the density matrix. Since

$$\rho_{m,m}(\mathrm{final}) = \sum_n U_{mn}\rho_{n,n}(\mathrm{initial})U^{\dagger}_{nm} = \sum_n |U_{mn}|^2 \rho_{n,n}(\mathrm{initial}) \ , \tag{25}$$

this evolution rule relates to diagonal elements before and after each subresonance. We, therefore, require only the magnitudes of the subresonance evolution operators.

While we must calculate the *complex* evolution ma-

trices through each subresonance, between subresonances only the diagonal elements of the density matrix survive. Hence the final diagonal matrix to be obtained results from the successive multiplication of matrices formed by the *magnitudes* of the elements of successive subresonance evolution matrices.

Suppose the initial density matrix is labeled $\rho(0)$ and the final, following the $2j+1$ subresonances, by $\rho(2j+1)$, then

$$\rho_{m,m}(2j+1)=\sum_n |U_{m,n}^{1\to 2j+1}|^2\rho_{n,n}(0) \tag{26}$$

where

$$|U_{n,m}^{\alpha\to\gamma}|^2=\sum_k |U_{nk}^{\beta\to\gamma}|^2 |U_{km}^{\alpha\to\beta}|^2 . \tag{27}$$

The calculation of the final density matrix thus depends only on the determination of the subresonance evolution operators for the separate submanifolds.

In the rotating frame, the Hamiltonian matrix for the $|m-1\rangle$, $|m\rangle$, $|m+1\rangle$ submanifold is given by Eq. (19) as

$$\mathcal{H}_{m,m\pm1}=\begin{bmatrix} -\hbar\gamma B_0+\hbar\omega+P2m+\frac{1}{3}P & -\hbar\gamma B_1\frac{1}{2}k_m\cos(\omega_m t) & 0 \\ -\hbar\gamma B_1\frac{1}{2}k_m\cos(\omega_m t) & -\frac{2}{3}P & -\hbar\gamma B_1\frac{1}{2}k_{m-1}\cos(\omega_m t) \\ 0 & -\hbar\gamma B_1\frac{1}{2}k_{m-1}\cos(\omega_m t) & \hbar\gamma B_0-\hbar\omega-P2m+\frac{1}{3}P \end{bmatrix} .$$

The rf frequency may be centered with respect to subresonance to yield

$$\mathcal{H}'_{m,m\pm1}=\begin{bmatrix} \hbar\omega+\frac{1}{3}P & -\hbar\gamma B_1\frac{1}{2}k_m\cos(\omega_m t) & 0 \\ -\hbar\gamma B_1\frac{1}{2}k_m\cos(\omega_m t) & -\frac{2}{3}P & -\hbar\gamma B_1\frac{1}{2}k_{m-1}\cos(\omega_m t) \\ 0 & -\hbar\gamma B_1\frac{1}{2}k_{m-1}\cos(\omega_m t) & -\hbar\omega+\frac{1}{3}P \end{bmatrix} .$$

Note that ω refers to the frequency of the suppressed carrier.

In the limit that $\omega_m\to 0$ the 2×2 submatrices of the 3×3 Hamiltonian reduce to that of the pseudo-spin half case treated previously for unmodulated single passage in which the effective rf field is $k_m B_1$. For $\omega_m\neq0$ the role of the $\frac{1}{2}k_m$ factor in $\mathcal{H}'_{m,m\pm1}$ deserves comment. In our pseudo-spin-1 formalism it appears that the effective rf field is halved. This is indeed the case since for carrier suppressed amplitude modulation the sidebands have each one-half the amplitude of the carrier at zero modulation. In MAPON our measure of the intrinsic excitation linewidth is therefore $\frac{1}{2}B_1\overline{k_m}$ if the linearly polarized applied rf field is $2B_1\cos(\omega t)\cos(\omega_m t)$.

C. Influence of the manifold quantum number j

The subresonance U matrices will vary between nuclear spin systems to the extent that k_m values differ. Spin systems encountered in NMR ON may have large angular momentum quantum numbers j. (^{60}Co is the classic NMR ON system for which $j=5$). The manifold j value is significant in two respects. First, the higher the value of j the better the adiabaticity of the sweep, as we have already noted. Second, there is a difference in overall cyclic reorganization between integral and half-integral j as is apparent in Fig. 7. This difference arises at the *actual* "line center." When $\omega_m=P/\hbar$ under these circumstances the population redistribution in the three-level submanifolds corresponds to a pseudo-spin-1 inversion. For half-integral j this leads to a cyclic shift identical to the case at $\omega_m>P/\hbar$. For integral j the order of the cyclically shifted populations is inverted as shown in Fig. 7(b). This differing final order of the first two accessed populations leads to subtle differences in the B_ν parameters with B_4 being much more sensitive to this order than B_2. The details of these differences are exhibited in the calculations to follow. When the highest energy states are accessed first [$(d\omega/dt)P<0$] the order of these lowest populations is largely irrelevant for highly orient-

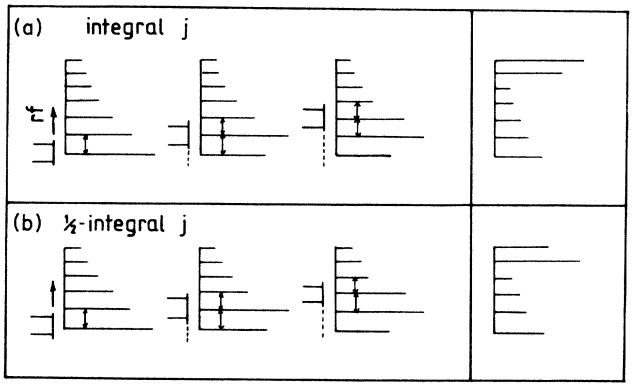

FIG. 7. Modulated adiabatic passage through subresonances for the case $\omega_m=P/\hbar$ in which pseudo-spin-1 inversions may be envisaged. The case for integral j is shown in (a). (b) The case of half-integral j is illustrated, and here the reorganization is identical to the asymptotic result for $\omega_m>P/\hbar$. The sweep direction is "reverse" and most populated levels accessed first, and the observed difference in cyclic reorganization is significant. For the "forward" sweep (not shown) the difference involves the final order of the least populated levels, and the result for $\omega_m=P/\hbar$ is practically identical to the $\omega_m>P/\hbar$ asymptote. In this case any ordering difference arising from integral or half-integral j is masked.

ed nuclei whether of half-integral or integral spin. Since this particular sweep sense yields the largest postpassage MAPON signal, it corresponds to the practical case, and we refer to it as the "forward sweep." However, in the reverse sweep direction we assert that the MAPON signal dependence on j for $\omega_m \geq P/\hbar$ is significant but largely confined to B_4 effects. This point is illustrated in the calculations to follow.

Of course the particular details of the MAPON signal depend on the relative weightings of B_2 and B_4. Therefore, the MAPON lineshape will depend on the $U_\nu F_\nu$ coefficients of the particular nuclear decay and on the initial parent spin temperatures. However, in general, the practical consequence of the similarity of the $\omega_m = P/\hbar$ and $\omega_m > P/\hbar$ redistributions is that the *signal* line center suffers a small shift to lower modulation frequency by $\frac{1}{2}\gamma B_1 \overline{k_m}$. $\overline{k_m}$ is an "internal average" which takes into account the various subresonances of the complete MAPON sweep through a given isochromat.

In choosing numerical parameters appropriate for the calculation of the evolution matrices we are bound by time constraints. The time taken to perform the numerical calculations depends particularly on the choice of experimental adiabatic parameter A, where

$$A = (\gamma B_1)^2/(d\omega/dt) \ . \tag{28}$$

For high-adiabaticity calculations we have chosen $A = 8$. We will be concerned with high-spin nuclei such as ^{60}Co ($j = 5$) for which $\frac{1}{2}k_m$ values range between 2.74 and 1.58. For $j = 5$ and $A = 8$ we certainly satisfy the high-adiabaticity condition $A_m \gg 1$ for each subresonance. We also investigate the influence of integral and nonintegral spin by comparing the dependence of B_2 and B_4 on ω_m for $j = 5$ and $j = \frac{9}{2}$.

D. Numerical calculations

Numerical evaluation of the U matrix in successive incremental approximations requires a choice of the time step size δt and the starting frequency ω. Since resonant excitations occur at $\omega = \pm(P/\hbar - \omega_m)$, it is appropriate to sweep from $-P/\hbar$ to $P/\hbar$. The sweep should then start far from excitation provided $P/\hbar \gg \gamma B_1 k_m$. This is exactly the subresonance separation condition which applies in the MAPON experiment.

More difficult is the choice of δt. We must use a power-series expansion for $\exp(-i\mathcal{H}'_{m,m\pm1}t)$ in the numerical calculation, and so δt must be kept sufficiently small for an accurate expansion with finite numbers of terms. However, $\delta\omega/\delta t$ is fixed by the desired adiabatic parameter. In order to achieve large A values, δt may not be made arbitrarily small else the frequency step becomes too small and the number of successive matrix multiplications diverges.

The test to apply for the quality of the numerical evaluation is the unitarity of the evolution operator. For the overall unitarity to be kept to within 2%, we find the maximum step δt to be $8\times10^{-6}(\gamma B_1)^{-1}$ for a first-order exponential expansion and $4\times10^{-3}(\gamma B_1)^{-1}$ for a second-order expansion. No advantage is achieved by adopting a higher order expansion since δt would then be sufficiently large that the phase step $\omega_m \delta t$ becomes too coarse.

A convenient choice of parameter is given by $P/\hbar = 16\gamma B_1$ with ω_m being varied from $P/\hbar - 5\gamma B_1$ to $P/\hbar + 5\gamma B_1$ in order to adequately sample the line shape. For $A = 8$ we thus require 6×10^4 incremental steps per subresonance in order to satisfy the unitarity condition. This proves excessive for most computers. In fact, the effective adiabatic parameter increases away from subresonance, so it is possible to sweep more rapidly "at the edges." We employ a sweep rate which varies as the off-resonance displacement raised to the power $\frac{3}{2}$. This reduces the number of incremental steps by nearly 2 orders of magnitude without introducing significant errors. A calculation for one MAPON sweep at high adiabaticity ($A = 8$) through the $j = 5$ manifold took 1.5 days using an 8086-based P.C. programmed in BASIC. The time taken decreases for lower values of A.

The result of a sweep through the subresonance centered on $m = -4$ is shown in Table I for $A = 8$ and modulation frequencies of $\omega_m = P/\hbar - 5\gamma B_1, P/\hbar, P/\hbar + 5\gamma B_1$. The accuracy (as measured by the unitarity of U) is sufficiently good to enable successive multiplication without introducing significant errors. The end subresonances involving two sublevels only are evolved incrementally in an entirely similar manner using a 2×2 representation of the pseudo-spin-$\frac{1}{2}$ manifold.

Figure 8 shows the high adiabaticity postpassage change in B_2 and B_4 as the modulation frequency is varied for both $j = 5$ and $j = \frac{9}{2}$. We have chosen a starting population difference corresponding to a Zeeman level separation of 160 MHz at $T = 10$ mK. This particular Zeeman splitting corresponds to ^{60}Co*Fe*. While some differences are apparent, the two spin manifolds show a broadly similar response with the line center shifted slightly below $\omega_m = P/\hbar$. The complicated lineshape, especially apparent for B_4, reflects the tensorial nature of the detection process. It is clear that the change in B_2 and B_4 for $\omega_m \geq P/\hbar$ is effectively constant for the forward sweep. For the reverse sweep B_4 shows a significant difference between $\omega_m = P/\hbar$ and $\omega_m \gg P/\hbar$ for the integral j whereas for the half-integral j the change in B_4 as $\omega_m \gg P/\hbar$ should be asymptotic to the change at $\omega_m = P/\hbar$. In fact, because a finite adiabatic

TABLE I. $|U_{mn}|^2$ matrices for the pseudo-spin-1 submanifold centered on $m = -4$ for the case $A = 8$.

ω_m			
$P/\hbar - 5\gamma B_1$	0.002	0.952	0.055
	0.003	0.054	0.952
	1.000	0.003	0.002
$P/\hbar$	0.001	0.007	0.998
	0.023	0.972	0.007
	0.977	0.024	0.001
$P/\hbar + 5\gamma B_1$	0.013	0.010	0.993
	0.941	0.046	0.017
	0.049	0.948	0.006

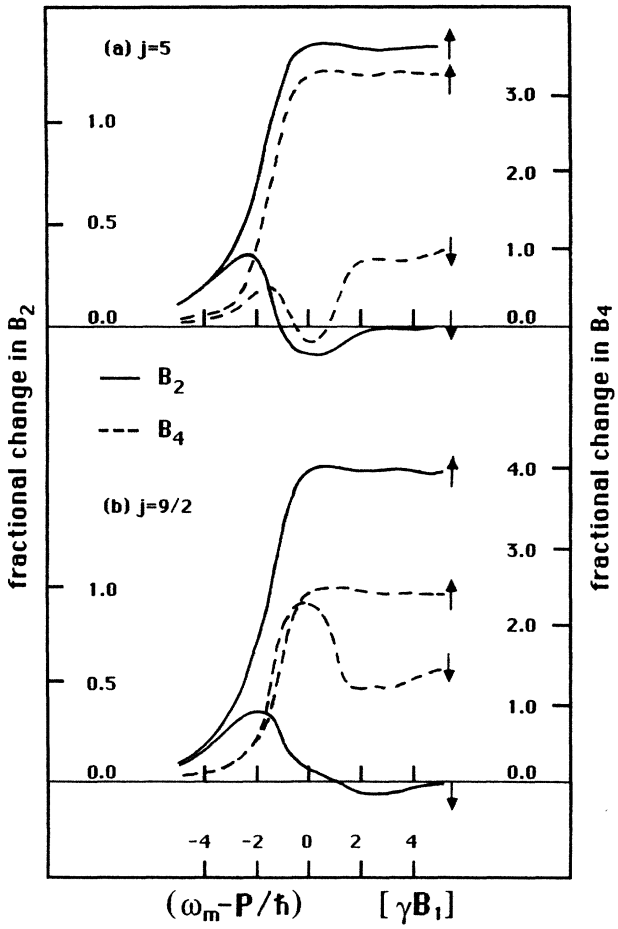

FIG. 8. Fractional changes in B_2 (solid line) and B_4 (broken line) for forward (↑) and reverse (↓) MAPON sweeps. ω_m is expressed in units of γB_1. (a) The result for j integral exhibits a clear difference in response between $\omega_m = P/\hbar$ and $\omega_m > P/\hbar$ for the case of reverse sweep only. (b) The result for half-integral j should be identical at $\omega_m = P/\hbar$ to the asymptotic result for $\omega_m > P/\hbar$. $A = 8.0$, $T = 12.5$ mK, $\gamma B_0 = 10^9$ s^{-1}.

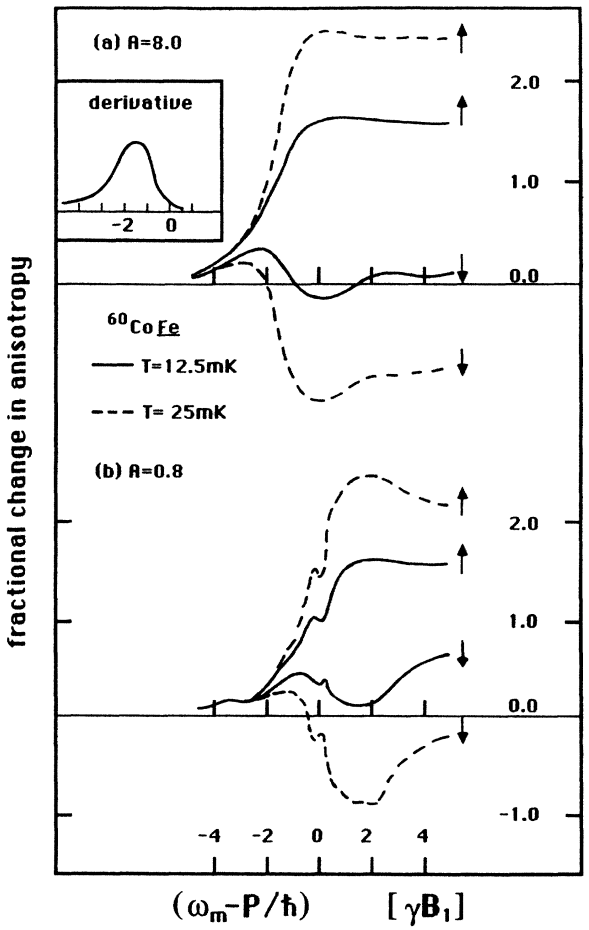

FIG. 9. MAPON response as a function of modulation frequency for $^{60}CoFe$ under differing conditions of temperature and adiabaticity. (a) $A = 8$ and $T = 12.5$ mK and 25 mK; (b) $A = 0.8$ and $T = 12.5$ mK and 25 mK. A clear effect is apparent in the vicinity of $\omega_m = P/\hbar$ irrespective of temperature or adiabatic parameter. For $A \gg 1$ a small shift of the line center is apparent. The line shape derivative is shown in the inset to (a).

parameter is used a degree of population mixing occurs between the population pair transported right across the manifold. This causes an imperceptible effect for the forward sweep where this pair corresponds to the least populated levels. In the reverse sweep, however, the mixing leads to the small discrepancy in B_2 and the larger discrepancy in B_4 apparent in Fig. 8.

Figure 9 shows the overall MAPON response curves for the full γ anisotropy exhibited by $^{60}CoFe$ under varying conditions of adiabaticity and temperature. In practice the signal differences between forward and reverse sweeps may not be so great. The effect of relaxation during the finite time taken to sweep through an inhomogeneously broadened line will inevitably modify the anisotropy change apparent in Fig. 9. These effects are explored in the subsequent paper.[20]

Where the adiabaticity is low, the line shape is exceedingly complex, and the line center shift by $\frac{1}{2}\gamma B_1 k_m$ is no longer apparent. Despite the line shape complexity where $A < 1$, it is clear that a determination of P by the MAPON technique does not depend on high adiabaticity let alone a knowledge of the value of A appropriate to the nuclear ensemble. In each case shown there is a clear crossover in postpassage signal in the vicinity of $\omega_m = P/\hbar$.

Of course, the most desirable line shape corresponds to $A \gg 1$. The derivative of the postpassage response is shown in Fig. 9(a), and while not the classic Lorentzian line shape, it suffices for the purpose of establishing the value of $P/\hbar$ with a FWHM of order $\frac{1}{2}\gamma B_1 \overline{k_m}$ and with a line center offset of $\frac{1}{2}\gamma B_1 \overline{k_m}$. Our fundamental broadening is now the natural linewidth of nuclear magnetic resonance.

We note that the line center offset may provide a means of calibrating internally enhanced radiofrequency fields for those broadline impurity systems where B_1 cannot be determined by ensemble rotation using pulsed NMR ON. This approach does require that the electric field gradient distribution is sharp compared with $\frac{1}{2}\gamma B_1 \overline{k_m}$.

IV. CONCLUSION

The technique of Modulated Adiabatic Passage of Oriented Nuclei offers a means of directly measuring quadrupole splittings much smaller than the inhomogeneous magnetic broadening. The quadrupole spectroscopy is performed in the domain of the modulation frequency. It is superposed on the adiabatic passage NMR experiment and has the full sensitivity of NMR ON. Indeed the MAPON postpassage signal is considerably larger than anisotropy destruction of order 100% associated with cw NMR ON and some 40% larger than the optimum postpassage signal of unmodulated single passage NMR ON.[18]

A key feature of the method is the coupling of three levels by two rf fields, thus transforming the evolution in the spin manifold to a sequence of pseudo-spin-1 interactions. In consequence we effectively observe the single quadrupole splitting associated with $j=1$ and avoid the complication of multiple harmonics familiar for spin echoes suffering quadrupole modulation[26] in high-spin manifolds.

The MAPON technique promises to be of particular use in elucidating the small electric quadrupole interactions associated with light nuclear impurities in ferromagnets. In particular it offers a means of systematically obtaining accurate magnitudes and signs of very small electric field gradients, along with their distribution, and in a manner which is easy to interpret.

ACKNOWLEDGMENT

We acknowledge the assistance of Dr. W. D. Hutchison in checking our calculations.

APPENDIX: RANK-2 CARTESIAN TENSORS FOR SPIN 1

Spin operators used as a basis for the density matrix in pseudo-spin 1 as employed in Eqs. (18) and (19) are given as follows:

$$T_{zz}=\frac{1}{\sqrt{6}}(3J_z^2-2)\ ,$$

$$T_{xz}=\frac{1}{\sqrt{2}}(J_zJ_x+J_xJ_z)\ ,$$

$$T_{yz}=\frac{1}{\sqrt{2}}(J_zJ_y+J_yJ_z)\ ,$$

$$\frac{1}{\sqrt{3}}(T_{xx}-T_{yy})=\frac{1}{\sqrt{2}}(J_x^2-J_y^2)\ ,$$

$$T_{xy}=\frac{1}{\sqrt{2}}(J_xJ_y+J_yJ_x)\ .$$

[1]E. Matthias and R. J. Holliday, Phys. Rev. Lett. **17**, 897 (1966).
[2]P. Herzog, Hyperfine Interact. **8**, 215 (1980).
[3]G. Gehring and H. C. W. L. Williams, J. Phys. F **4**, 291 (1974).
[4]E. Hagn, Hyperfine Interact. **22**, 19 (1985).
[5]P. D. Johnston and N. J. Stone, J. Phys. C **5**, L303 (1972).
[6]E. Hagn, K. Leuthhold, E. Zech, and H. Ernst, Phys. Lett. **85B**, 321 (1979).
[7]E. Hagn, K. Leuthold, E. Zech, and H. Ernst, Z. Phys. A **295**, 385 (1980).
[8]P. T. Callaghan, P. D. Johnston, W. M. Lattimer, and N. J. Stone, Phys. Rev. B **12**, 3526 (1975).
[9]P. T. Callaghan, W. M. Lattimer, P. D. Johnston, and N. J. Stone, Hyperfine Interact. **2**, 288 (1976).
[10]E. Hagn and E. Zech, Phys. Rev. A **307**, 159 (1982).
[11]E. Hagn and E. Zech, Phys. Rev. B **29**, 1148 (1984).
[12]J. J. Spijkerman, J. C. Travis, D. N. Pipkorn, and C. E. Violet, Phys. Rev. Lett. **76**, 323 (1971).
[13]E. Hagn, Phys. Rev. B **25**, 1521 (1982).
[14]E. Hagn and E. Zech, Phys. Rev. B **25**, 1529 (1982).
[15]I. Solomon, Phys. Rev. **110**, 61 (1958).
[16]G. V. H. Wilson, D. H. Chaplin, P. Cooke, H. R. Foster, and P. Lynam, Aust. J. Phys. **30**, 461 (1971).
[17]C. G. Don, Ph.D. thesis, Monash University, Australia, 1972.
[18]P. T. Callaghan, P. D. Johnston, and N. J. Stone, J. Phys. C **7**, 3161 (1974).
[19]P. T. Callaghan, W. M. Lattimer, N. J. Stone, and P. D. Johnston, Hyperfine Interact. **2**, 291 (1976).
[20]P. J. Back, D. H. Chaplin, and P. T. Callaghan, following paper, Phys. Rev. B **37**, 4911 (1988).
[21]R. J. Blin-Stoyle and M. A. Grace, Handb. Phys. **42**, 555 (1957).
[22]*Low Temperature Nuclear Orientation*, edited by H. Postma and N. J. Stone (North-Holland, Amsterdam, 1986).
[23]A. Abragam, *The Principles of Nuclear Magnetism* (Oxford University, London, 1961).
[24]N. J. Stone, Hyperfine Interact. **8**, 83 (1980).
[25]W. M. Lattimer, Ph.D. thesis, Oxford University, 1976.
[26]H. Abe, H. Yasuoka, and A. Hirai, J. Phys. Soc. Jpn. **21**, 77 (1966).